

## Study on Magnetic Force Calculation of Spherical Permanent Magnets

Yuyang Zhang<sup>1</sup>, Yonggang Leng<sup>1\*</sup>, Dan Tan<sup>2</sup>, and Jinjun Liu<sup>3</sup>

<sup>1</sup>*School of Mechanical Engineering, Tianjin University, Tianjin 300350, China*

<sup>2</sup>*Beijing Institute of Nanoenergy and Nanosystems, Chinese Academy of Sciences, Beijing 100083, China*

<sup>3</sup>*School of Control and Mechanical Engineering, Tianjin Chengjian University, Tianjin 300384, China*

(Received 14 June 2018, Received in final form 5 December, Accepted 12 December 2018)

**This paper presents three approaches to calculate the interacting magnetic force about spherical permanent magnet, respectively based on magnetic dipole-dipole model, equivalent magnetic charge model and equivalent magnetizing current model. We use all of three models to fully calculate and study the behaviors of lateral and axial forces with respect to the related positions between a pair of spherical magnets. The accuracies of the calculation results are compared with the experimental data. In conclusion, the magnetic dipole-dipole model has the most advantageous accuracy and efficiency for the magnetic force calculation about spherical permanent magnets on account of the particularity of sphere. Our study provides an important criterion for choosing a proper method to calculate magnetic force about spherical permanent magnet.**

**Keywords :** spherical permanent magnet, magnetic force calculation, magnetic dipole-dipole, equivalent magnetic charge, equivalent magnetizing current

### 1. Introduction

Spherical permanent magnet is always applied in some mechanical structures and frontier researches such as end-effector for robotic magnetic manipulation, flexible chain or ring, magnetic abrasive finishing and some vibration energy harvester [1-4], because the unique characteristics of point-contact and uniform magnetization. Therefore, an accurate magnetic force calculation method about spherical permanent magnet is essential to predict and analyze the behaviors of components or structures with spherical permanent magnets participating. This paper presents three equivalent models, magnetic charge, magnetizing current and magnetic dipole-dipole, which are used to calculate the interacting magnetic force between two spherical permanent magnets.

In this paper, we first set up the experiment to measure the actual forces interacted between two same spherical permanent magnets. Then, we use all of three models to fully calculate the interacting magnetic force and study

the behaviors of lateral and axial forces respectively with respect to the lateral displacement and interval between magnets. Subsequently, we compare the accuracies of three models with experimental measurement data to confirm the most accurate and effective model. Moreover, the applicability of the magnetic dipole-dipole model is also discussed.

### 2. Experiment

First of all, we design an experiment to measure the actual position-dependent magnetic forces between a pair of  $\phi 30$  mm Y30BH spherical permanent magnets, as shown in Fig. 1. One magnet of the pair is attached to the adjusted platform and the other one to a dynamometer (HF-5), the relative position of spherical magnets is adjusted with screws of platform. We read the relative displacements of spherical magnet by laser displacement sensor (LK-G5001V) and record the forces with the dynamometer, respectively, whose minimum resolutions are 0.001 mm and 0.001 N.

In order to obviously observe the accuracies of magnetic force calculation with the three models, in this paper, we just measure the interacting axial forces (AF)  $F_z$  and lateral forces (LF)  $F_L$  when one magnet is moving over another fixed one along the x-axis, as shown in Fig. 2,

©The Korean Magnetism Society. All rights reserved.

\*Corresponding author: Tel: +86(0)2227403285

Fax: +86(0)2227403285, e-mail: leng\_yg@tju.edu.cn

This paper was presented at the IcaUMS2018, Jeju, Korea, June 3-7, 2018.

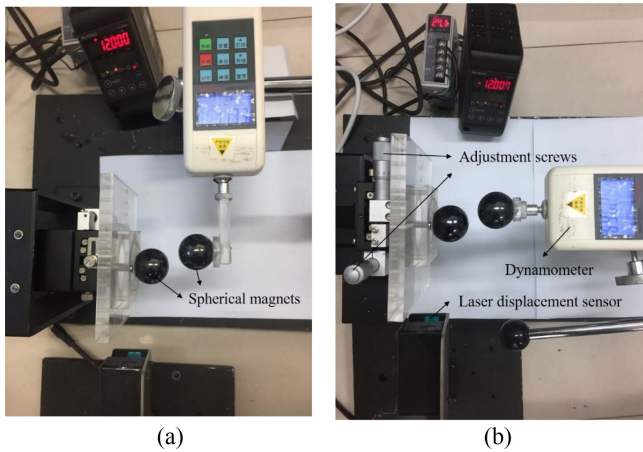


Fig. 1. (Color online) Magnetic force measurement system. (a) lateral force, (b) axial force.

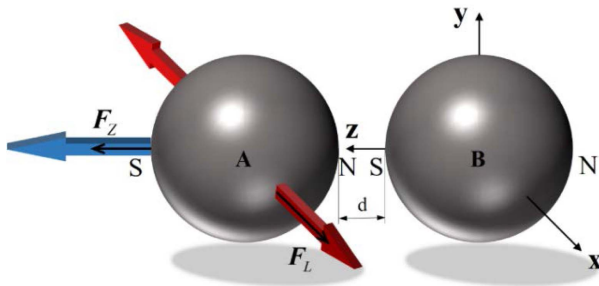


Fig. 2. (Color online) Schematic of the spherical magnet moving state.

where the magnet B is fixed and the magnet A is movable. Moreover, when the projections of the pair of spherical magnets coincide in z-direction, we change the interval  $d$  and record the axial magnetic forces. That means the interacting magnetic forces' values we achieve are plotted with respect to the displacement  $x$  and interval  $d$  respectively. The experimental data are plotted as dots in Fig. 6 and compared with the simulation results based on the calculations in the later section to evaluate the accuracies of models.

### 3. Magnetic Force Calculation Models

#### 3.1. Magnetic dipole-dipole model

The theory of magnetic dipole-dipole treats two interacting spherical permanent magnets as a pair of magnetic dipoles with directional magnetic moments  $\mu = MV$ , as shown in Fig. 3, where  $M$  is the magnetization intensity of permanent magnet and  $V = \frac{4}{3}\pi R^3$  represents the volume of magnet,  $R$  is the radius of spherical magnet. The magnetic induction intensity produced by magnet B on an arbitrary point A is

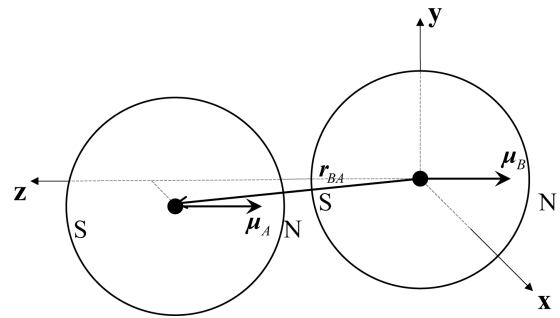


Fig. 3. Schematic drawing of magnetic dipole-dipole model.

$$\mathbf{B}_{BA} = -\frac{\mu_0}{4\pi} \nabla \frac{\boldsymbol{\mu}_A \cdot \mathbf{r}_{BA}}{\|\mathbf{r}_{BA}\|_2^3}, \quad (1)$$

where  $\mathbf{r}_{BA}$  represents the vector pointing to A from B,  $\mu_0$  is the permeability of vacuum.

The interacting magnetic force is obtained by solving the Maxwell equations with the introduction of a scalar magnetic potential  $U_m = -\mathbf{B}_{BA} \cdot \boldsymbol{\mu}_B$  [5]:

$$\mathbf{F} = -\nabla U_m. \quad (2)$$

Subsequently, the lateral magnetic force in x-direction is written as

$$F_L = -\frac{3\mu_0\mu_A\mu_B}{4\pi r_{BA}^4} \left[ \left( 1 - 5 \frac{z^2}{r_{BA}^2} \right) \frac{x}{r_{BA}} \right], \quad (3)$$

and the axial magnetic force in z-direction is

$$F_Z = -\frac{3\mu_0\mu_A\mu_B}{4\pi r_{BA}^4} \left( 3 \frac{z}{r_{BA}} - 5 \frac{z^3}{r_{BA}^3} \right), \quad (4)$$

where  $r_{BA} = (x^2 + z^2)^{1/2}$ ,  $z$  and  $x$  are the coordinates of magnet A's center point in coordinate system in which the center point of magnet B is chosen as the original point. Here, we define the attractive magnetic force as positive, the same hereinafter. So there are minuses in the front of formula (3) and (4).

#### 3.2. Equivalent magnetic charge model

The equivalent magnetic charge theory is based on the magnetic dipole model as its micro model, it believes that a magnetized permanent magnet has a north and a south pole on the two end faces on account of the organized interior magnetic dipolar molecules arranging orderly in the direction of magnetic field, of which the north and south poles link one after another and offset. Hence, positive and negative magnetic charges only distribute on the surfaces of magnetic north and south poles [6]. The magnetic field produced by a permanent magnet can be equivalent to the field produced by these magnetic

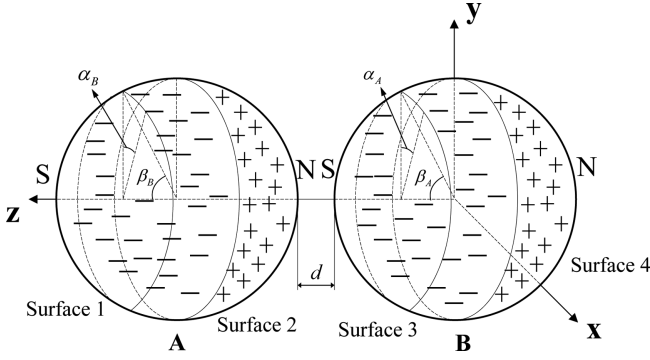


**Fig. 4.** Schematic drawing of equivalent magnetic charge model.

charges on the magnetic poles' semi-spherical surfaces, so can the magnetic force acting on permanent magnet. In other words, the interacted magnetic force between two spherical permanent magnets is summation of interacted magnetic force among those surface magnetic charges, as shown in Fig. 4.

Therefore, according to the magnetic charge theory, the interacting magnetic force between two spherical permanent magnets is calculated by using twice spherical surface integrals of the dipole-dipole model. We use  $\sigma_s$  to denote the surface charge density, the magnetic moments in Eqn. (2), (3) and (4) are in form of  $\mu = \sigma_s dS$ , and the surface charge density  $\sigma_s = M [7]$ .

Note that we define the serial number for every hemispherical surface in Fig. 4, the interacting force between two spherical permanent magnets is a summation of the contribution of both hemispherical magnetic pole surfaces of two permanent magnets:

$$F = \sum_{m=1}^2 \sum_{n=3}^4 F_{mn}, \quad (5)$$

where  $F_{mn}$  represents the interacting magnetic force between two hemispherical surfaces which belongs to different magnet:

$$F_{mn} = \pm \iint_S \frac{3\mu_0 M_A M_B}{4\pi r_{BA}^4} \left( \frac{x + R_A \sin \beta_A \sin \alpha_A - R_B \sin \beta_B \sin \alpha_B}{r_{BA}} \right) \left( 1 - 5 \frac{z_{mn}^2}{r_{BA}^2} \right) dS_A dS_B \mathbf{i} \pm \iint_S \frac{3\mu_0 M_A M_B}{4\pi r_{BA}^4} \left( \frac{3z_{mn}}{r_{BA}} - 5 \frac{z_{mn}^3}{r_{BA}^3} \right) dS_A dS_B \mathbf{k}, \quad (6)$$

$dS$  represents the infinitesimal cell area on the hemispherical surface, the parameters  $\beta$  and  $\alpha$  are shown in Fig. 4,  $R$  is the radius of spherical magnet. The  $z_{mn}$  in this equation is used to distinguish the interaction between different pairs of hemispherical surfaces numbered in Fig. 4 and these are:

$$z_{23} = d + R_A(1 - \cos \beta_A) + R_B(1 - \cos \beta_B), \quad (7)$$

$$z_{13} = d + R_A(1 - \cos \beta_A) + R_B(1 + \cos \beta_B), \quad (8)$$

$$z_{24} = d + R_A(1 + \cos \beta_A) + R_B(1 - \cos \beta_B), \quad (9)$$

$$z_{14} = d + R_A(1 + \cos \beta_A) + R_B(1 + \cos \beta_B). \quad (10)$$

For  $z_{14}$  and  $z_{23}$ , the signs in the front of Eqn. (6) are minus, for  $z_{13}$  and  $z_{24}$ , the signs are plus as same as the definition in dipole-dipole model.

According to the Eqns. (5)-(10), the axial and lateral interacting magnetic force between two spherical permanent magnets are simulated as plotted in Fig. 6. In this case, the magnetic force in y-direction is zero, the magnetic force in x-direction can represent the lateral force. By changing the coordinate system, we can calculate interacting magnetic force of the other relative positions between magnets, because of symmetry of sphere.

### 3.3. Equivalent magnetizing current model

The equivalent magnetizing current theory believes that every magnetic domain, the basic unit of a magnetic medium, can be equivalent to a micro ring current. An unmagnetized permanent magnet shows no magnetism on macro-scale because the directions of micro ring currents distribute random; whereas a magnetized permanent magnet has polarity due to micro ring currents arranged along the direction of the magnetic field. In the case of a uniformly magnetized spherical permanent magnet whose magnetization intensity  $M$  is constant [8], the internal adjacent magnetizing ring currents have inverse tangential directions and are offset by each other. Hence, only the surface magnetizing currents exist around the outmost surface of the spherical magnet, as shown in Fig. 5. The surface magnetizing current density is

$$K_m = M \times \hat{n}, \quad (11)$$

where  $\hat{n}$  is surface normal unit vector.

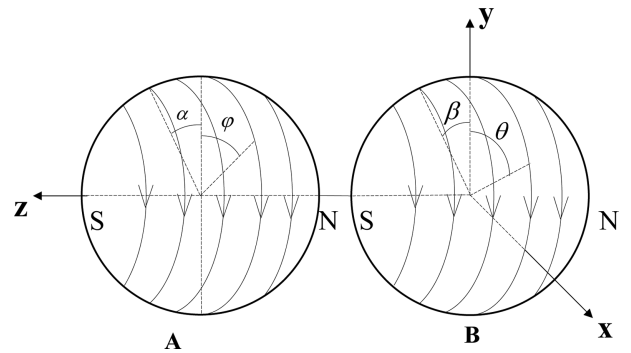


**Fig. 5.** Schematic drawing of equivalent magnetizing current model.

The magnetic force calculation of this double spherical magnet interacted system can be equivalent to that the currents on magnet A's surface is placed in the external magnetic field produced by the current of magnet B.

According to Biot-Savart law with some basic coordinate transformation, we first achieve the magnetic induction intensity of an arbitrary point  $P(x, y, z)$  in space produced by spherical magnet B:

$$\mathbf{B} = \frac{\mu_0 M_B}{4\pi} \int_{-\pi/2}^{\pi/2} R_B d\beta \int_0^{2\pi} \left( \frac{(z - R_B \sin \beta) R_B \cos \beta \cos \theta}{r^3} d\theta \mathbf{i} + \frac{(z - R_B \sin \beta) R_B \cos \beta \sin \theta}{r^3} d\theta \mathbf{j} - \frac{y R_B \cos \beta \sin \theta + x R_B \cos \beta \cos \theta - (R_B \cos \beta)^2}{r^3} d\theta \mathbf{k} \right), \quad (12)$$

where  $r^3 = \left( \begin{array}{l} (x - R_B \cos \beta \cos \theta)^2 \\ + (y - R_B \cos \beta \sin \theta)^2 \\ + (z - R_B \sin \beta)^2 \end{array} \right)^{3/2}$ ,  $R_B$  is the radius of

spherical magnet B, the meanings of  $\theta$  and  $\beta$  are shown in Fig. 5.

Subsequently, the magnetic force between two spherical permanent magnets is treated as the Ampere's force of magnetizing currents on the magnet A's surfaces in the field produced by currents of magnet B. we calculate the interacted magnetic force using Ampere's law,

$$\mathbf{F} = - \iint_S \mathbf{K}_{mA} \times \mathbf{B} ds, \quad (13)$$

where  $S$  represents the area of the surfaces where the currents are. Hence, the interacting magnetic force is expressed as:

$$\begin{aligned} \mathbf{F} = & \left[ M_A \int_{-\pi/2}^{\pi/2} R_A^2 \cos \alpha d\alpha \int_0^{2\pi} B_k (x + R_A \cos \alpha \cos \varphi, y \right. \\ & \left. + R_A \cos \alpha \sin \varphi, z + R_A \sin \alpha) \cos \varphi d\varphi \right] \mathbf{i} \\ & + \left[ M_A \int_{-\pi/2}^{\pi/2} R_A^2 \cos \alpha d\alpha \int_0^{2\pi} B_k (x + R_A \cos \alpha \cos \varphi, y \right. \\ & \left. + R_A \cos \alpha \sin \varphi, z + R_A \sin \alpha) \sin \varphi d\varphi \right] \mathbf{j} \\ & + \left[ M_A \int_{-\pi/2}^{\pi/2} R_A^2 \cos \alpha d\alpha \int_0^{2\pi} B_i (x + R_A \cos \alpha \cos \varphi, y \right. \\ & \left. + R_A \cos \alpha \sin \varphi, z + R_A \sin \alpha) \cos \varphi d\varphi \right. \\ & \left. + M_A \int_{-\pi/2}^{\pi/2} R_A^2 \cos \alpha d\alpha \int_0^{2\pi} B_j (x + R_A \cos \alpha \cos \varphi, y \right. \\ & \left. + R_A \cos \alpha \sin \varphi, z + R_A \sin \alpha) \sin \varphi d\varphi \right] \mathbf{k}. \end{aligned} \quad (14)$$

where the meanings of  $\alpha$  and  $\varphi$  are also shown in Fig. 5,  $R_A$  represents the radius of spherical magnet A.

## 4. Simulation and Comparison

Based on the above calculation, we simulate the interacting magnetic force between two spherical permanent magnets with MATLAB. The lateral and axial force's curves with respect to lateral displacement and interval are separately plotted in Fig. 6 and compared with the experiment data measured. The interval  $d$  is set as 8 mm and the permeability of vacuum  $\mu_0 = 4\pi \times 10^{-7}$  H/m. The magnetization intensities  $M$  of the above three methods are respectively set as  $2.81 \times 10^5$  A/m (dipole-dipole),  $2.6 \times 10^4$  A/m (charge) and  $3.1 \times 10^5$  A/m (current). Some researchers proposed and proved the equivalence of these three models in micro scale [9, 10]. For a pair of magnetic dipoles (charges) and two micro magnetizing loop current, the expressions of interactions have unique form with the same magnetization intensities. However, in the

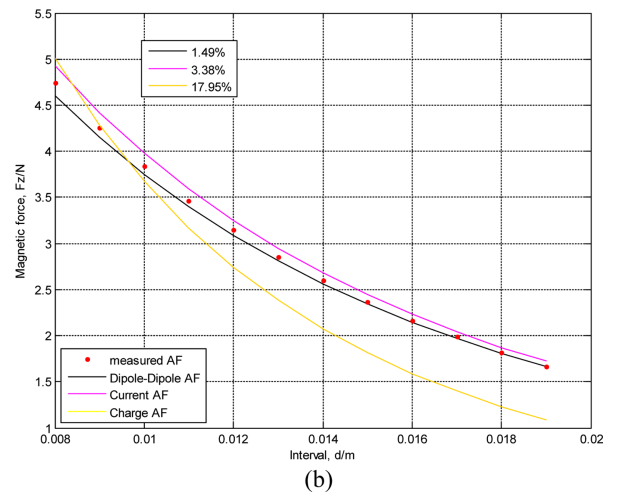
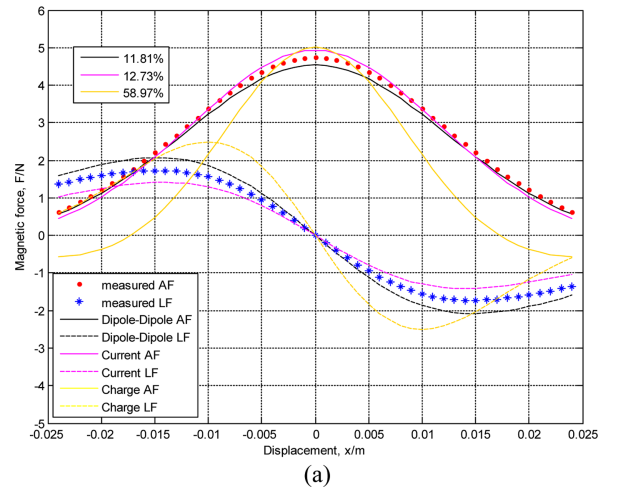


**Fig. 6.** (Color online) Comparison of simulation results of different models with the experiment data. (a) lateral and axial force with respect to displacement  $x$ ; (b) axial force with respect to interval  $d$ .

most of cases of the magnetic force calculation between permanent magnet, the magnets have macro scales. Different integral paths of the three calculation methods lead to different values of magnetization intensities. As our paper shows, the dipole-dipole model does not need any integral operation as the micro form of magnetic charge model; the method of equivalent magnetizing current is a kind of line integral calculation of current path focusing on the outermost loop where the macro equivalent currents distribute; the calculation based on the theory of magnetic charge is a kind of surface integral of magnetic pole faces where the equivalent magnetic charges distribute.

Comparing different calculation expressions of magnetic force models, the magnetizations intensity  $M$  are independent of integral and could be put in the head or end of the formula as constants in the case of uniformly magnetized spherical permanent magnets. The value of magnetization intensity makes no difference in the general shape of simulation curve as functions of any abscissa parameter  $x$  or  $d$  because of the linear relation between magnetization intensity and interacting magnetic force, it only decides the magnitude of magnetic forces.

Therefore, we just assign the values of magnetization based on an empirical basis in the former literature and try the best to make the most of measured values consistent with the curves. Concretely, we calculate the variances of absolute error between every simulated and measured value with different magnetization intensity. By comparing the variance, we confirm the final magnetization intensity when the variance is minimum.

We also calculate the average relative errors:

$$\bar{E}_r = \frac{\sum_{i=1}^N \left| \frac{\Delta F_i}{F_{ei}} \right|}{N}, \quad (15)$$

where the  $\Delta F_i$  in the Eqn. (10) represents the absolute error of every force's value, and there is  $\Delta F_i = F_{ei} - F_{si}$ , where  $F_{ei}$ ,  $F_{si}$  and  $N$  respectively represent the measured value, simulated value and the quantity of the values which contains both axial and lateral forces. The results of each case are also marked in the Fig. 6.

## 5. Conclusion

It's observed from Fig. 6 that the equivalent magnetizing current model and magnetic dipole-dipole model almost

have similar better accuracies than that of magnetic charge model. Moreover, considering the process of modelling and calculation, the magnetic dipole-dipole model is much simpler to be established to calculate the interacting magnetic force and can be the first choice to calculate magnetic force about spherical permanent magnet. Although it has been verified that magnetic dipole-dipole model isn't appropriate for the cubic or cylindrical magnet due to the specific shape of permanent magnet which dipole model cannot describe [11], it is suitable for the calculation of magnetic force interacted between spherical permanent magnets, because dipole can be treated as sphere in topology.

## Acknowledgment

This work was financially supported by the National Natural Science Foundation of China (Grant No. 51675370) and the Tianjin Research Program of Application Foundation and Advanced Technology (Grant No. 15JCZDJC32200).

## References

- [1] S. E. Wright, A. W. Mahoney, K. M. Popek, and J. J. Abbott, IEEE International Conference on Robotics and Automation (2015) pp 1190-1195.
- [2] C. L. Hall, D. Vella, and A. Goriely, *Mathematics* **73**, 6 (2013).
- [3] B. Han, C. Deng, and Y. Chen, *Tribology* **33**, 6 (2013).
- [4] S. D. Moss, J. E. Mcleod, I. G. Powlesland, and S. C. Galea, *Sen. Act. A Phys.* **175**, 2 (2012).
- [5] K. W. Yung, P. B. Landecker, and D. D. Villani, *Magn. Elec. Sep.* **9**, 1 (1998).
- [6] M. F. J. Kremers, D. T. E. H. V. Casteren, J. J. H. Paulides, and E. A. Lomonova, Tenth International Conference on Ecological Vehicles and Renewable Energies. IEEE (2015) pp 1-7.
- [7] N. Sadowski, Y. Lefèvre, M. Lajoie-mazenc, and J. P. A. Bastos, *J. Phys. III.* **2**, 5 (1992).
- [8] J. S. Agashe and D. P. Arnold, *J. Phys. D Appl. Phys.* **41**, 10 (2008).
- [9] H. Zan, M. S. thesis, Xi'an University of Architecture and Technology, Xi'an (2008).
- [10] T. Kovanen, T. Tarhasaari, and L. Kettunen, *IEEE Trans. Magn.* **48**, 13 (2012).
- [11] Y. Zhang, Y. Leng, and S. Fan, International Design Engineer Technology Conference, Cleveland (2017) pp 67168.